J Nanopart Res (2013) 15:1745
DOI 10.1007/s11051-013-1745-8

RESEARCH PAPER

Gold nanoparticles trigger apoptosis and necrosis in lung cancer cells with low intracellular glutathione

Min Liu · Xiaohu Gu · Ke Zhang · Yi Ding · Xinbing Wei · Xiumei Zhang · Yunxue Zhao

Received: 29 November 2012 / Accepted: 22 May 2013 / Published online: 30 July 2013

Abstract Previously 13 nm gold nanoparticles (GNPs) have been shown to display cytotoxicity to lung cancer cells when L-buthionine-sulfoximine (BSO) was used to decrease the expression of intracellular glutathione (GSH). In this study, we investigated how the GNPs induced cell death at the molecular level. Dual staining with fluorescent annexin V, and propidium iodide was used to discriminate apoptotic and necrotic cell death. We found that GNPs induced apoptosis and necrosis in lung cancer cells with low level of intracellular GSH. The disruption of F-actin and phosphorylation of H2AX induced by GNPs were both associated with apoptosis. The ER stress was caused, mitochondrial membrane potential was disrupted, intracellular calcium was elevated and intracellular caspase-3 was activated by GNPs in lung cancer cells with low intracellular GSH, while cell death could not be prevented by the pan-caspase inhibitor *N*-benzyloxycarbonyl-Val-Ala-Asp-fluoromethylketone. The cells were further examined for caspase-independent death. After GNPs and BSO exposure, apoptosis inducing factor, endonuclease G, and glyceraldehyde-3-phosphate dehydrogenase translocated into the nuclei of apoptotic cells. Receptor-interacting protein 1 kinase inhibitor necrostatin-1 significantly decreased the PI positive cells that were induced by GNPs and BSO. Taken together, our results suggest that multiple modes of cell death are concurrently induced in GNPs-exposed lung cancer cells with low intracellular GSH, including apoptosis and necrosis. These results have important implications for GNPs in anticancer applications.

Keywords Gold nanoparticles · Glutathione · Apoptosis · Necrosis

M. Liu · K. Zhang · X. Wei · X. Zhang (✉) · Y. Zhao (✉)
Department of Pharmacology, School of Medicine, Shandong University, Jinan 250012, People's Republic of China
e-mail: zhangxm@sdu.edu.cn

Y. Zhao
e-mail: zhaoyunxue@sdu.edu.cn

X. Gu · Y. Ding
School of Chemistry and Chemical Engineering, Shandong University, Jinan 250100, People's Republic of China

Introduction

Nanotechnology provides a flexible platform for the development of effective therapeutic nanomaterials (Mura and Couvreur 2012). Various nanomaterials have been extensively utilized in medical applications including local drug delivery, cell imaging, and biosensors (Ambrogio et al. 2011; Erathodiyil and Ying 2011; Ho et al. 2011). Therefore, understanding the influence of nanomaterials on live cell functions, controlling such effects, and using them for disease

therapeutics are now principal aims and among the most challenging aspects of nanobiotechnology and nanomedicine. Gold nanoparticles (GNPs) have attracted much interest for their novel properties and potential biological applications. Due to their straightforward synthesis and stability and the easy modification of their functional groups allowing the targeting of certain properties, significant research efforts have been conducted with a view to develop application of GNPs in biomedical applications, such as biological imaging (Kim et al. 2010), gene and drug delivery (Hu et al. 2010; Lu et al. 2010; Xia et al. 2011), and cancer treatments (Dreaden et al. 2012; Kang et al. 2010; Minelli et al. 2010; Shukla et al. 2012). However, their toxicological issues are still under debate and the molecular mechanism underlying the interactions of GNPs and cells remains to be elucidated (Alkilany and Murphy 2010; Khlebtsov and Dykman 2011; Li and Chen 2011). In our previous study, GNPs (13 nm) have been shown to induce cell death to lung cancer cells when L-buthionine-sulfoximine (BSO) was used to decrease the expression of intracellular glutathione (GSH) (Zhao et al. 2011). Apoptosis and necrosis are two major cell death modalities (Krysko et al. 2008; Zhang et al. 2009). The apoptotic process is mainly executed by a class of cysteine proteases known as caspases, which can be sorted into intrinsic and extrinsic apoptotic pathway. Extrinsic pathway involves triggering of death receptors, which induces the activation of the initiator caspase-8/-10 in the death-inducing signaling complex followed by direct cleavage of downstream effector caspases, including caspase-3 and caspase-7. After activation of the intrinsic mitochondrial pathway, the release of mitochondrial cytochrome *c* initiates apoptosome-formation with initiator caspase-9, and subsequent activation of caspase-3 and caspase-7 (Kaufmann et al. 2008; Vucic et al. 2011). On the other hand, apoptosis inducing factor (AIF) and endonuclease G (EndoG) can be released from mitochondria into the cytosol, which be translocated to the nucleus and then cleave DNA independent of caspase activation (Norberg et al. 2010; Saelens et al. 2004; Van Loo et al. 2001). Necrosis was considered an abrupt and uncontrolled type of cell death. However, recent evidence clearly shows that necrosis also involves elaborate molecular circuitry. Recent study has shown that necrotic cell death is highly regulated by the Receptor-interacting protein 1 (RIP1) and RIP3 kinases. Programmed necrosis can be initiated by several stimuli including DNA damage, oxidative stress, infection, and activation of pattern recognition receptors (Fortes et al. 2012; Krysko et al. 2008; Zhang et al. 2009).

Cancer remains a major threat to public health (Umar et al. 2012). There is accumulating evidence that targeting multiple cell death pathways may be an advantageous strategy for treating cancer (Hu and Xuan 2008; Speirs et al. 2011). Our previous studies showed that GNPs generated more intracellular reactive oxygen species (ROS) in lung cancer cells with low intracellular GSH (Zhao et al. 2011). At higher concentrations, ROS often cause cellular damage and lead to cell death, including apoptosis and necrosis (Hahm et al. 2011; Nair et al. 2009; Morgan and Liu 2010; Steinbrenner and Sies 2009). The impressive results in our previous study and the potential applications of GNPs in anticancer research encourage elucidating the type of cell death and underlying cytotoxic mechanism of GNPs in lung cancer cells. Kang et al. (2010) reported that GNPs with nuclear targeting motifs elicit significant damage of DNA and concomitant apoptosis in human oral squamous cell carcinoma. However, Pan et al. (2009) found that GNPs with 1.4 nm in diameter triggered necrosis by oxidative stress and mitochondrial damage in HeLa cervix carcinoma epithelial cells. In the present study, we showed that GNPs induce cell death by activating multiple death pathways, including apoptotic signaling pathway and necrotic pathway in lung cancer cells with low intracellular GSH.

Materials and methods

Materials

Chloroauric acid ($HAuCl_4 \cdot 4H_2O$, A.R.), ascorbic acid (AA, A.R.), potassium citrate (TPC) (K_3C_6–H_5O_7 $3H_2O$, A.R.), and concentrated nitric acid (HNO_3, 67 %, A.R.) were purchased from Shanghai Sinopharm Chemical Reagent Co. Ltd. TRITC–phalloidin, BSO, Necrostatin-1 (Nec-1), and reduced GSH, were purchased from Sigma-Aldrich. Annexin-V FITC apoptosis kit was purchased from Invitrogen. Nuclear extract kit, DAPI, and Fluo-3/AM were purchased

from Beyotime Institute Biotechnology. The caspase inhibitor *N*-benzyloxycarbonyl-Val-Ala-Asp-fluoromethylketone (zVAD-fmk) was purchased from Promega. Cleaved caspase-3 (Asp175) rabbit pAb (Alexa Fluor® 488 conjugate), Phospho-Histone H2AX (Ser139) rabbit mAb (Alexa Fluor® 488 conjugate), Histone H3 (3H1) rabbit mAb (HRP conjugate), Bcl-2 rabbit mAb, Bip rabbit mAb, Puma rabbit pAb, Bax rabbit mAb, GAPDH XP® rabbit mAb (HRP conjugate), AIF XP® rabbit mAb, and EndoG rabbit pAb, were purchased from Cell Signaling Technology. p53 rabbit pAb and CHOP rabbit pAb were purchased from Bioworld Technology. β-actin rabbit pAb was purchased from Beijing Biosynthesis Biotechnology Co. Ltd.

Synthesis of GNPs

Gold nanoparticles were synthesized using the well-known wet-chemical reduction method, as described previously (Zhao et al. 2011). Typically, 100 ml 1 mM $HAuCl_4$ aqueous solution was heated to boiling for 5 min. Upon the introduction of 10 mL 40 mM TPC solution, the mixed solution was kept boiling for another 15 min and then allowed to cool to room temperature naturally. GNPs precipitates were collected by centrifugation and rinsed with ultrapure water for three times, and then the product was dispersed in 4 mM TPC solution and kept at 4 °C for further use.

Cell culture

Lung cancer cells (A549 cells) were purchased from Shanghai Cell Bank, Type Culture Collection Committee, Chinese Academy of Sciences. The cells were cultured in F12K medium supplemented with 10 % heat inactivated FBS, 2 mM glutamine, 100 U/ml penicillin, and 100 μg/ml streptomycin, and maintained at 37 °C in a humidified atmosphere of 5 % CO_2.

Analysis of cell apoptosis and necrosis

The ability of GNPs to induce cell apoptosis and necrosis of A549 cells was quantified by annexin V and PI staining and flow cytometry, as described previously (Zhao et al. 2010). Briefly, after treatment with GNPs (10 μM) and BSO (0.5 mM) for 72 h, cells were collected and washed with PBS twice, and subjected to annexin V and propidium iodide staining using annexin-V FITC apoptosis kit following the step-by-step protocol provided by the manufacturer. After staining, flow cytometry was performed for the quantification of apoptotic and necrotic cells.

Immunofluorescence and confocal microscopic analysis for actin filaments

F-actin of A549 cells was detected using fluorescent phalloidin and analyzed by confocal microscopy, as described previously (Zhao et al. 2010). Cells were seeded to the glass coverslips in cell culture dishes (3.5 cm) overnight. GNPs (10 μM) and BSO (0.5 mM) were then added and cells were cultured for 48 h. After fixing with 4 % paraformaldehyde, cells were treated with 0.1 % Triton X-100 and blocked with 1 % BSA. Cells were incubated with TRITC-conjugated phalloidin for 60 min and examined under Confocal Laser Scanning Microscope (40×, oil).

Mitochondrial membrane potential assay

JC-1(5,50,6,60-tetrachloro-1,10,3,30-tetraethylbenzamidazolocarbocyanin iodide) is most widely applied for detecting mitochondrial depolarization occurring in the early stages of apoptosis. Mitochondrial membrane potential ($\Delta\Psi_m$) analysis was conducted and modified, as described previously (Zhao et al. 2010). Briefly, A549 cells were treated with GNPs (10 μM) and BSO (0.5 mM) for 48 h, at the end of treatment, cells were harvested. Cells were incubated with JC-1 at 37 °C for 20 min. Stained cells were washed with PBS twice and analysed by flow cytometry.

Measurement of intracellular free Ca^{2+}

Intracellular free Ca^{2+} levels in A549 cells were measured using Ca^{2+} specific fluorescent probe Fluo-3/AM, as described recently with minor modifications (Wen et al. 2011). A549 cells were treated with GNPs (10 μM) and BSO (0.5 mM) for 48 h, at the end of treatment, cells were harvested. Cells were loaded with 5 μM Fluo-3/AM for 60 min at room temperature. After incubation, cells were harvested and washed twice with PBS and analyzed by flow cytometry.

Confocal microscope for DNA damage test

γ-H2AX of A549 cells was detected using fluorescent conjugate anti-γ-H2AX antibody by confocal microscopy, as described previously (Burma et al. 2001). Cells were seeded to the glass coverslips in cell culture dishes (3.5 cm) overnight. GNPs (10 μM) and BSO (0.5 mM) were then added, and cells were cultured for 48 h. After fixing with 4 % paraformaldehyde, the cells were treated with 0.1 % Triton X-100 and blocked with 1 % BSA. Then, cells were incubated with Alexa Fluor 488 conjugate anti-γ-H2AX antibody for 1 h. Cells were washed with PBS and then stained with 4,6-diamidino-2-phenylindole (DAPI). Fluorescence images were captured by Confocal Laser Scanning Microscope (63×, oil).

Measurement of intracellular cleaved caspase-3

Intracellular cleaved caspase-3 was determined by flow cytometry with cleaved caspase-3 (Asp175) antibody. After treatment with GNPs (10 μM) and BSO (0.5 mM) for 48 h, the cells were trypsinized, collected by centrifugation, washed twice with PBS, and fixed with 4 % paraformaldehyde. After treated with 0.1 % Triton X-100 and blocked with 1 % BSA, cells were incubated with cleaved caspase-3 (Asp175) antibody (Alexa fluor 488 conjugate) for 30 min. Stained cells were washed with PBS twice and analysed by flow cytometry.

Western blot analysis

Cells were washed twice with ice-cold PBS and lysed with RIPA buffer containing protease inhibitors. After centrifugation at 13,000×*g* for 15 min, protein concentrations of the lysates were determined by the micro-BCA protein assay kit. The total cellular protein extracts were boiled with 5× Laemmli sample buffer and separated by SDS-PAGE and transferred to PVDF membrane. Membranes were blocked with 5 % non-fat dry milk in TBS containing 0.1 % Tween 20 for 1 h at room temperature and incubated with appropriate antibodies overnight at 4 °C. Blots were washed three times in TBS-T buffer, followed by incubation with the appropriate HRP-linked secondary antibodies for 1 h at room temperature. The specific proteins in the blots were visualized using the enhanced chemiluminescence reagent.

Nuclei isolation

Isolation of nuclei was carried out using the nuclear extract kit according to the manufacturer's protocol. Translocation of AIF, EndoG and GAPDH to the nucleus was analyzed by western blot. Briefly, after treatment with GNPs (10 μM) and BSO (0.5 mM) for 48 h, cells were trypsinized, collected by centrifugation and washed with PBS. Cell pellets were resuspended in hypotonic buffer and incubated for 15 min at 4 °C. Cells were permeabilized with detergent and centrifuged (5 min, 13,000×*g*, 4 °C) and the supernatants were removed (nonnucleic fraction). Pellets were resuspended in lysis buffer, incubated for 30 min at 4 °C, and centrifuged (10 min, 13,000×*g*, 4 °C). The supernatants contain the nuclear proteins.

Statistical analysis

The statistical analysis was done using Student's *t* test with the SPSS 16.0 statistical program. $p < 0.05$ was accepted as significant, and $p < 0.01$ was regarded as highly significant.

Results

GNPs induce apoptosis and necrosis in lung cancer cells with low intracellular GSH

We have previously shown that if the GSH level is low in lung cancer cells, the GNPs can induce cell death (Zhao et al. 2011). We further tested whether, apoptosis and necrosis induction may contribute to the cytotoxicity function of GNPs in cancer cells. The ability of GNPs to induce apoptosis and necrosis in A549 cells with low intracellular GSH was thus evaluated by treatment of cells with GNPs (10 μM) and BSO (0.5 mM) for 72 h. And the cells were subsequently subjected to staining with annexin-V FITC(A), propidium iodide (PI), and flow cytometry analysis, in which A(−)/PI(−) cells are viable cells, A(+)/PI(−) are early apoptotic cells, A(+)/PI(+) are late apoptotic cells (known also as secondary necrosis), and A(−)/PI(+) are necrotic cells (Huang et al. 2011). As shown in Fig. 1a, b, GNPs (10 μM) and BSO (0.5 mM) treatment for 72 h caused 30.46 % annexin V-positive cells as compared to controls, which showed only 0.61 % annexin V-positive cells.

The results suggest that GNPs can induce apoptosis in lung cancer cells with low intracellular GSH. Annexin V-FITC/PI double staining by FACS showed that the population of A(−)/PI(+) stained cells, which usually is considered as primary necrosis, was also increased in BSO and GNPs-treated cells (Fig. 1a, c). The A(−)/PI(+) stained cells were detected at 8.39 % as compared to controls showing 2.28 %. The population of total PI positive cells, which comprises apoptosis and necrosis, was also significantly increased in BSO and GNPs-treated cells (Fig. 1a, d). In the presence of BSO or GNPs themselves, no apparent apoptosis and necrosis were observed (Fig. 1a–d). These results suggest that GNPs induce not only apoptosis, but also necrosis in A549 cells with low intracellular GSH.

GNPs induce actin depolymerization in lung cancer cells with low intracellular GSH

Previously we reported that GNPs can change the cell morphology, and induce cell death in lung cancer cells with low intracellular GSH (Zhao et al. 2011). It is well established that actin polymerization, which leads to F-actin assembly, and depolymerization plays a crucial role in cell morphological features. Alterations in actin organization and dynamics also play a role in apoptosis (Franklin-Tong and Gourlay 2008; Papadopoulou et al. 2008). In an attempt to explore the molecular events in response to treatment with GNPs in lung cancer cells with low intracellular GSH, the formation of actin cytoskeleton in A549 cells was assessed by staining with TRITC-phalloidin, which specifically binds F-actin. As shown in Fig. 2, F-actin assembly in A549 cells was disrupted by GNPs (10 μM) and BSO (0.5 mM). In contrast, only in the presence of GNPs or BSO themselves did not lead to influence on F-actin structure in A549 cells. The results indicate that GNPs can inhibit the actin polymerize, and then induce apoptosis in A549 cells with low intracellular GSH.

GNPs disrupt mitochondrial membrane potential in lung cancer cells with low intracellular GSH

The damage of mitochondrial integrity and the consequent loss of mitochondrial membrane potential ($\Delta\Psi_m$) is an early event in the initiation and activation of apoptotic and necrotic cascades (Landes and Martinou 2011; Ni et al. 2012). To determine whether GNPs induce mitochondrial disruption in A549 cells, we examined the depolarization of mitochondrial membrane by measuring the fluorescence remission shift (red to green) of the $\Delta\Psi_m$ sensitive cationic JC-1 dye in A549 cells. Cells were treated with GNPs (10 μM) and BSO (0.5 mM) for 48 h, and subsequently processed and stained with JC-1 dye and analyzed by flow cytometry. GNPs and BSO treated cells showed an increase in green/red fluorescence intensity indicating increased mitochondrial membrane depolarization (Fig. 3). The results indicate that the induction of apoptosis and necrosis by GNPs in lung cancer cells are closely associated with mitochondrial membrane disruption.

GNPs induce intracellular Ca^{2+} elevation in lung cancer cells with low intracellular GSH

Calcium overload can induce cell apoptosis and necrosis (Rasola and Bernardi 2011; Santo-Domingo and Demaurex 2010). Our results have shown that GNPs disrupt mitochondrial function and induce apoptosis and necrosis. To determine the role of calcium signaling in GNPs-induced apoptosis and necrosis, A549 cells were treated with GNPs (10 μM) and BSO (0.5 mM) for 48 h. Subsequently, Ca^{2+} was measured with a calcium indicator dye, Fluo-3/AM. We found that treatment with GNPs and BSO resulted in an elevation of Ca^{2+} in the cells (Fig. 4). The results suggest that GNPs-induced apoptosis and necrosis might be associated with its induction of Ca^{2+} elevation.

Histone H2AX is phosphorylated during GNPs-induced apoptosis of lung cancer cells

One of the early steps in the cellular response to DNA double-strand breaks (DSBs) is the phosphorylation of serine-139 of H2AX, a subclass of eukaryotic histone proteins that are part of the nucleoprotein structure called chromatin. It has been previously reported that the treatment of human cells with apoptosis-inducing agents results in the phosphorylation of histone H2AX during the initiation of DNA fragmentation (Burma et al. 2001; Mukherjee et al. 2006). Using a fluorescently-labeled antibody specific for the phosphorylated form of H2AX (γ-H2AX), discrete nuclear foci can be visualized at the sites of DSBs. We attempted to establish that GNPs (10 μM) and BSO (0.5 mM)

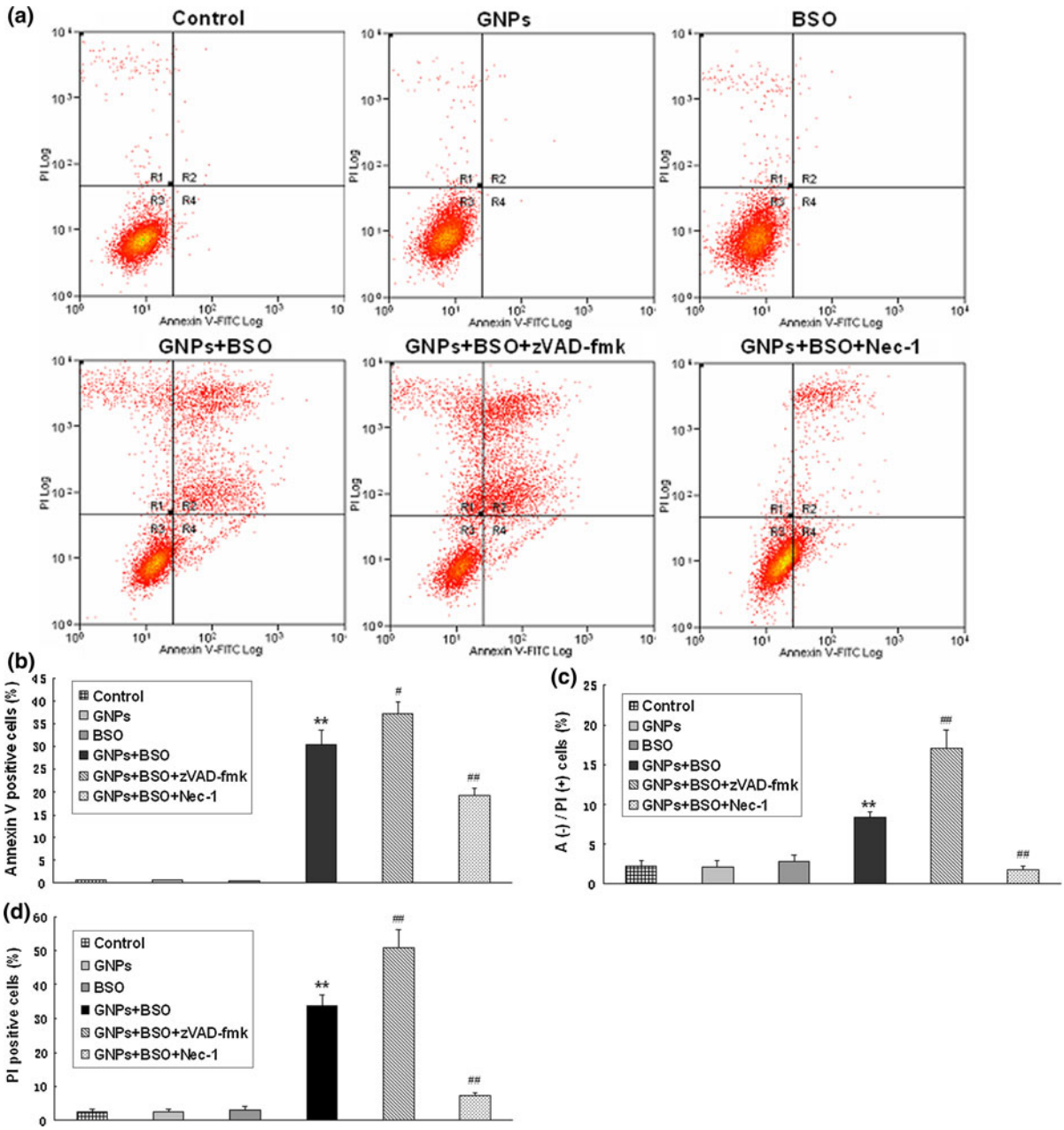

Fig. 1 Flow cytometric analysis of cells stained with Annexin V-FITC and PI. The A549 Cells were treated with GNPs (10 μM), BSO (0.5 mM), GNPs (10 μM) + BSO (0.5 mM), GNPs (10 μM) + BSO (0.5 mM) + zVAD-fmk (10 μM) or GNPs (10 μM) + BSO (0.5 mM) + necrostatin-1 (Nec-1, 20 μM) for 72 h, and then harvested and processed by annexin V-FITC and PI staining followed by flow cytometry analysis. **a** The fluorescence pattern of annexin V-FITC and PI-stained A549 cells after 72 h treatment. **b** Percentages of Annexin V positive cells for different treatments. **c** Percentages of PI positive and annexin V negative cells. **d** Percentages of PI positive cells for different treatments. Each *bar* represents the mean (±SD $n = 3$). $^{**}p < 0.01$, comparing with control. $^{\#}p < 0.05$, $^{\#\#}p < 0.001$, comparing with GNPs (10 μM) + BSO (0.5 mM)

treatment of A549 cells results in the induction of γ-H2AX. A549 cells were treated with GNPs and BSO and assayed 48 h later for H2AX phosphorylation by immunofluorescence staining with Alexa Fluor 488 conjugate anti-γ-H2AX antibody. As shown in Fig. 5, the treatment of A549 cells with GNPs and BSO

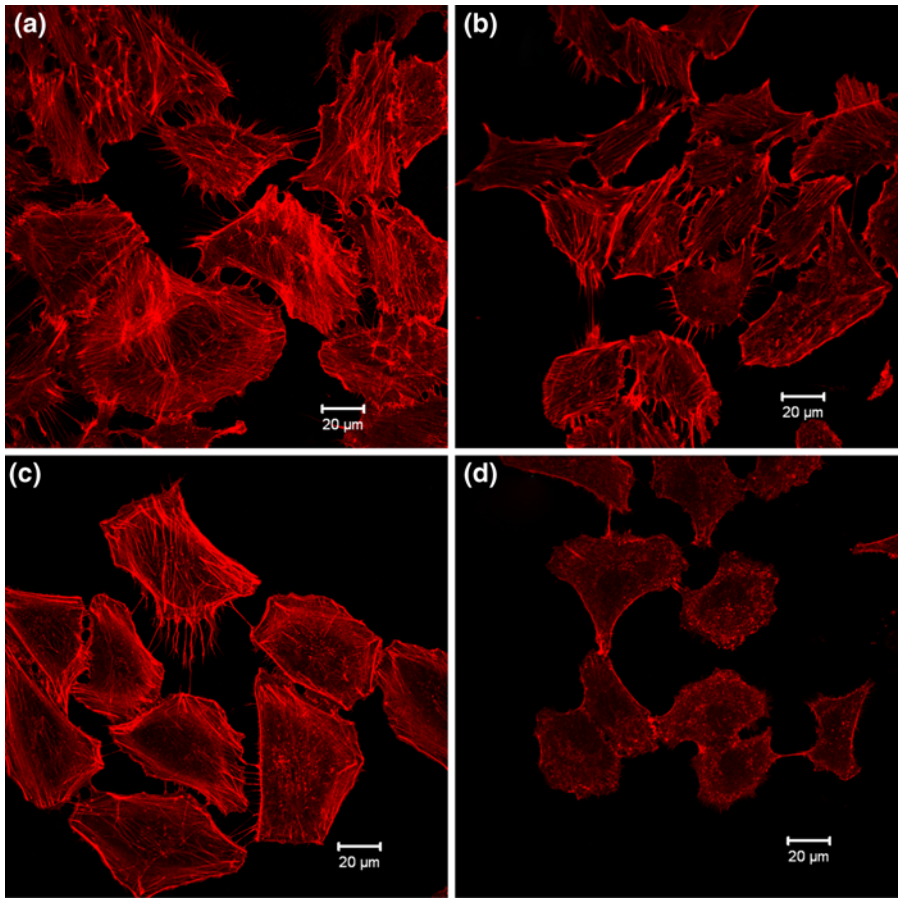

Fig. 2 Effect of GNPs on F-actin in A549 cells with low intracellular GSH. The A549 cells were treated with control (**a**), GNPs (10 μM) (**b**), BSO (0.5 mM) (**c**) or GNPs (10 μM) + BSO (0.5 mM) (**d**) for 48 h. The F-actin was detected by TRITC–phalloidin. Each group was tested in triplicate and the representative data are shown

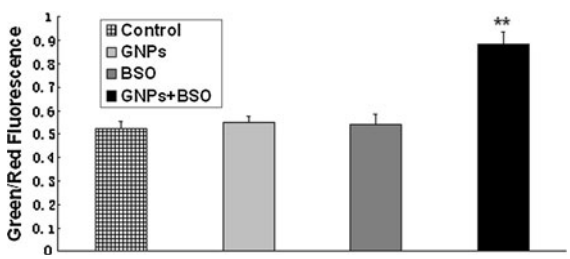

Fig. 3 Effect of GNPs on mitochondrial membrane potential in human A549 cells with low intracellular GSH. Cells were treated with GNPs (10 μM), BSO (0.5 mM) or GNPs (10 μM) + BSO (0.5 mM) for 48 h, and then harvested and processed by JC-1 staining followed by flow cytometry analysis. Each *bar* represents the mean (±SD, $n = 3$). $^{**}p < 0.01$, comparing with control

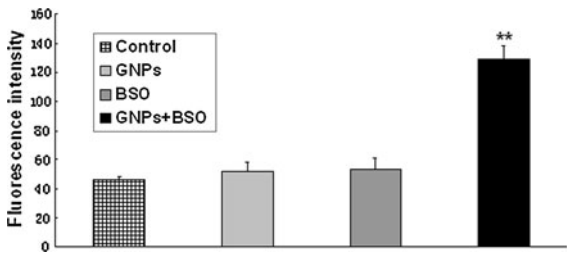

Fig. 4 Effect of GNPs on intracellular free Ca^{2+} ($[Ca^{2+}]i$) in A549 cells. The A549 cells were treated with GNPs (10 μM), BSO (0.5 mM) or GNPs (10 μM) + BSO (0.5 mM). After 48 h, cells were then harvested and stained with Fluo-3/AM. The fluorescence intensity was determined with flow cytometry. Each *bar* represents the mean (±SD) of triplicate determinations. $^{**}p < 0.01$ versus control

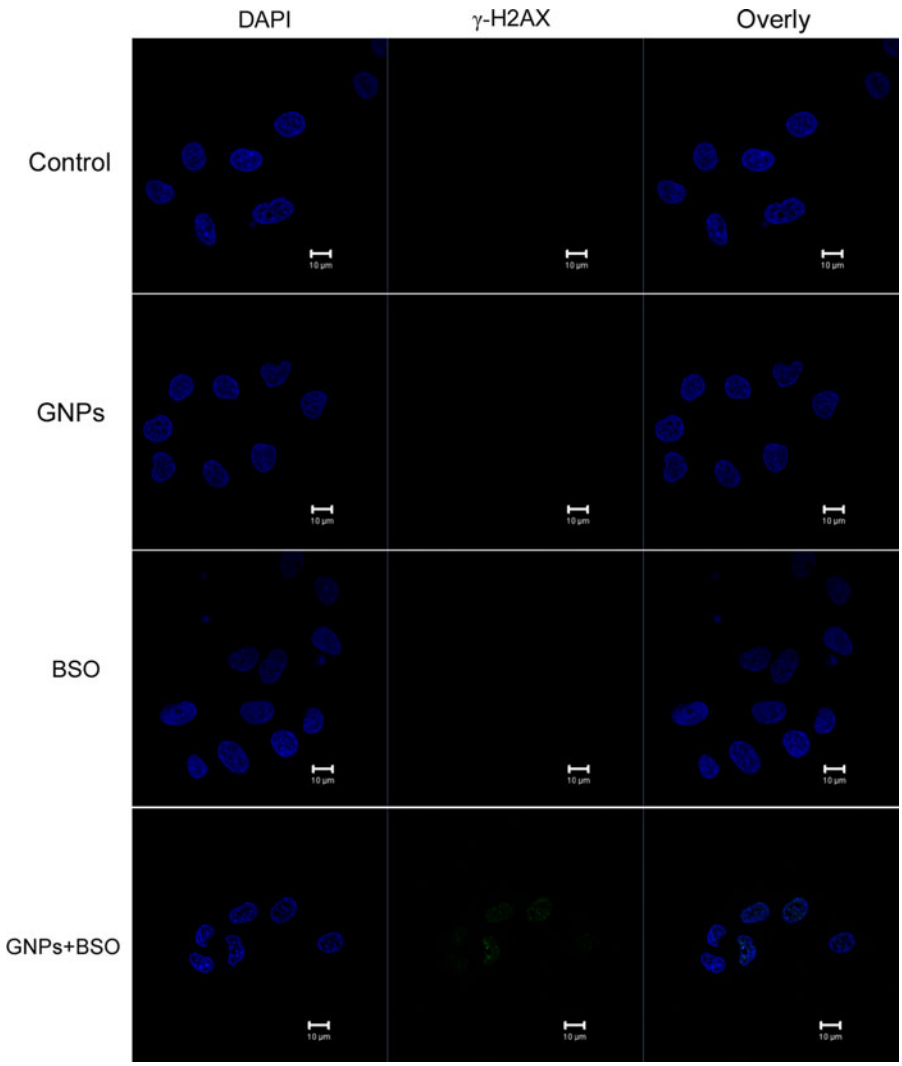

Fig. 5 Histone H2AX phosphorylation in GNPs-treated A549 cells with low intracellular GSH. A549 cells were treated with GNPs (10 μM), BSO (0.5 mM) or GNPs (10 μM) + BSO (0.5 mM) for 48 h, and immunostained with anti-γ-H2AX antibody (*green*). Nuclei were stained with 4,6-diamidino-2-phenphenylindole (DAPI) (*blue*). Each group was tested in triplicate and the representative data are shown. (Color figure online)

results in the phosphorylation of histone H2AX. The results indicate that DSBs are involved in GNPs induced cell apoptosis in lung cancer cells with low intracellular GSH.

GNPs cause activation of caspase-3 in lung cancer cells with low intracellular GSH

Detection of active caspase-3 in cells and tissues is an important method for apoptosis induced by a wide variety of apoptotic signals. Caspases are synthesized as inactive precursors or zymogens, which are activated by proteolytic cleavage to generate active enzymes that may further proteolytically cleave other caspases or cellular proteins. An active caspase consists of two large and two small subunits that form two heterodimers that associate in a tetramer. Activation of caspase-3 requires proteolytic processing of its inactive zymogen into activated p17 and p12 fragments (Mazumder et al. 2008; Nicotera 2002). To determine whether apoptosis induced by GNPs was a mitochondria-dependent caspase pathway, we examined the effects of the activation of caspase-3 by flow cytometry using specific antibodies that recognize the particularly cleaved and activated form after GNPs (10 μM) and BSO (0.5 mM) treatment. As shown in Fig. 6, increase in the cleaved and activated form of caspase-3 was observed in the treated cells as compared to the control cells. The results indicate that caspase activation is involved in GNPs induced cell apoptosis.

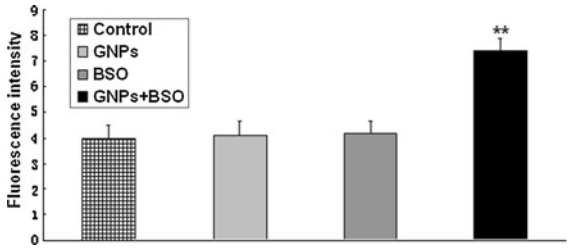

Fig. 6 Effect of GNPs on caspase-3 activation in A549 cells with low intracellular GSH. The A549 cells were treated with GNPs (10 μM), BSO (0.5 mM) or GNPs (10 μM) + BSO (0.5 mM) for 48 h. Cells were then harvested and stained with cleaved caspase-3 (Asp175) antibody (Alexa fluor 488 conjugate). The fluorescence intensity was determined with flow cytometry. Each *bar* represents the mean (±SD) of triplicate determinations. $^{**}p < 0.01$ versus control

zVAD-fmk can not inhibit cell death induced by GNPs in lung cancer cells with low intracellular GSH

zVAD-fmk is a cell-permeant pan caspase inhibitor that irreversibly binds to the catalytic site of caspase proteases and can inhibit induction of apoptosis (Weng et al. 2013; Zhang et al. 2012). To test if the increase in caspase-3 activity was necessary to trigger cell death, we employed the caspase inhibitor zVAD-fmk. Cells were cultured with GNPs and BSO (with or without zVAD-fmk at 10 μM) for 72 h. Then the cells were collected and stained with Annexin V and PI. Figure 1 shows that zVAD-fmk (10 μM) treatment did not decrease cell death in GNPs-treated cells. Furthermore, the cell death rate increased when cells were treated with GNPs (10 μM) and BSO (0.5 mM), in the presence of zVAD-fmk (10 μM) simultaneously compared with control (GNPs and BSO treated). The PI positive cell increased from 33.87 % (without zVAD-fmk) to 50.84 % (with zVAD-fmk). The annexin V positive cells increased from 30.46 % (without zVAD-fmk) to 37.15 % (with zVAD-fmk). The results indicate that GNPs induce cell death with a minor involvement of caspases.

GNPs induce ER stress in lung cancer cells with low intracellular GSH

The endoplasmic reticulum (ER) is an essential site of cellular homeostasis regulation, especially for the unfolded protein response (UPR). ROS have been reported to induce the UPR activation and ER stress (Verfaillie et al. 2012). In our previous study, we found that GNPs lead to an increase of intracellular ROS levels in lung cancer cells with low intracellular GSH. On the other hand, ER is main storage for intracellular Ca^{2+}, and stress can lead to the release of Ca^{2+} from its ER storage (Cao et al. 2013). We hypothesized that ER stress might be induced by the GNPs in A549 cells. To test this idea, we used western blot to examine the protein levels of two ER stress-responsive markers in the A549 cells. As depicted in Fig. 7, western blot analysis demonstrated a robust increase in the ER stress protein markers, including CHOP/GADD153 and BiP/GRP78, when the cells were treated with GNPs and BSO simultaneously. These results indicate that the occurrence of ER stress is involved in GNPs-induced cell death.

GNPs induced lung cancer cells apoptosis involves AIF and EndoG proapoptotic factors working independently of caspases

Apoptosis might proceed through the activation of both caspase-dependent and -independent pathways. The proapoptotic mitochondrial proteins AIF and EndoG are well-described death effectors working independently of caspases during cell death. On apoptotic stimuli, AIF and EndoG translate from mitochondria to the nucleus, inducing chromatin condensation and DNA fragmentation (Schneiders et al. 2009; Wang et al. 2012a, b). So the translocation of AIF and EndoG to the nucleus was analyzed by western blot. As shown in Fig. 8, the translocation of AIF and EndoG to the nucleus was detected after cotreatment of A549 cells with GNPs and BSO,

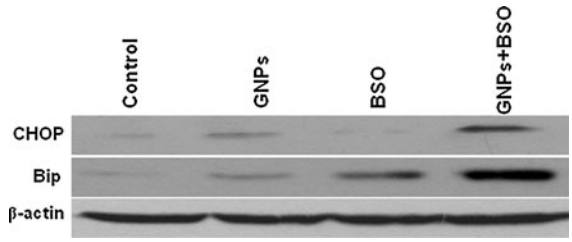

Fig. 7 Western blot analyses for levels of CHOP and Bip in A549 cells. The A549 cells were treated with GNPs (10 μM), BSO (0.5 mM), or GNPs (10 μM) + BSO (0.5 mM) for 48 h. Cell lysates were prepared from the treated cells, and western blot analyses were performed. β-actin was used as control. Each group was tested in triplicate and the representative data are shown

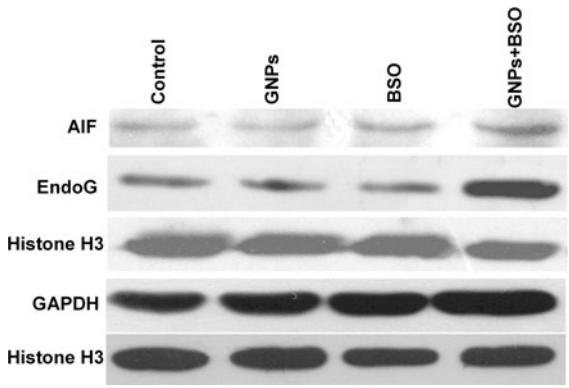

Fig. 8 Western blot analysis of nuclear fractions for AIF, EndoG, and GAPDH. Histone H3 is shown as loading control. The A549 cells were treated with GNPs (10 μM), BSO (0.5 mM), or GNPs (10 μM) + BSO (0.5 mM) for 48 h. Cells were then harvested and isolated the nuclei with nuclear extract kit. Western blot analyses were subsequently performed. Each group was tested in triplicate and the representative data are shown

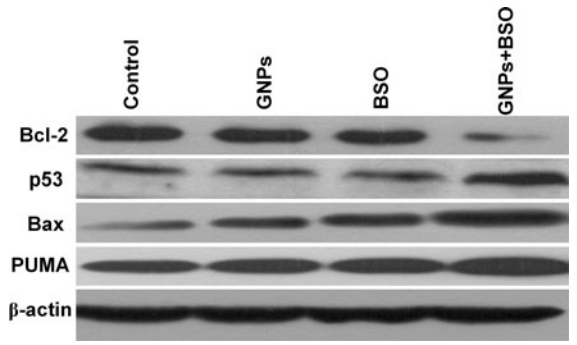

Fig. 9 Western blot analyses for levels of Bcl-2, p53, Bax, and Puma in A549 cells. The A549 cells were treated with GNPs (10 μM), BSO (0.5 mM) or GNPs (10 μM) + BSO (0.5 mM) for 48 h. Cell lysates were prepared from the treated cells, and western blot analyses were performed. β-actin was used as control. Each group was tested in triplicate and the representative data are shown

whereas, each treatment alone was not sufficient to stimulate the translocation of AIF and EndoG to the nucleus. These findings indicate that mitochondria-released proapoptotic proteins, AIF, and EndoG, are important factors in the GNPs-induced lung cancer cell apoptosis.

GNPs induced lung cancer cells apoptosis involves GAPDH

Glyceraldehyde-3-phosphate dehydrogenase (GAPDH) is an enzyme of glycolysis, and it is usually located in the cytosol. During apoptotic cell death, GAPDH translocates to the nucleus in a number of cell systems (Hara et al. 2005; Kim et al. 2009). GAPDH is a redox-sensitive enzyme and oxidative stress can stimulate its nuclear translocation (Dando et al. 2013). In our study, analysis of nuclear fractions revealed an accumulation of GAPDH in the nuclear fraction of GNPs and BSO cotreatment cells (Fig. 8), indicating that GAPDH nuclear accumulation is another factor in the GNPs-induced lung cancer cell apoptosis.

Effect of GNPs on expression of Bcl-2, p53, Bax, and Puma

To elucidate the molecular mechanisms involved in the observed apoptosis alterations, we investigated the effect of GNPs on the expression of proteins important for mitochondria mediated apoptosis. As shown in Fig. 9, the expression of Bcl-2 was found to be reduced in the cells with the cotreatment of GNPs (10 μM) and BSO (0.5 mM). In contrast, treating A549 cells with GNPs and BSO strongly induced the expression of p53, Bax, and PUMA.

Necrostatin-1 inhibits necrosis induced by GNPs in lung cancer cells with low intracellular GSH

Caspase inhibition sometimes shifts apoptosis to necrosis or enhances necrosis. Necrotic cell death is currently recognized to proceed in a programmed manner. Interruption of the signal transduction can reduce cell damage. An inhibitor, Nec-1, can attenuate the occurrence of necrotic cell death (Ma et al. 2011; Trichonas et al. 2010). Cell necrosis leads to the loss of membrane integrity and allows PI to diffuse into cells. Relative cell viability can thus be analyzed via the level of PI uptake. Nec-1 was therefore used to verify the damaging effect. As shown in Fig. 1, treatment with Nec-1 (20 μM) significantly suppressed the appearance of PI positive cells in GNPs and BSO treated cells, and Nec-1 also slightly affected Annexin V-positive cells. The PI positive cells decreased from 33.87 to 7.26 % (with Nec-1). The annexin V positive cells decreased from 30.46 to 19.23 % (with Nec-1). The results indicate that necrosis is an important death pathway of GNPs induced cell death in lung cancer cells with low intracellular GSH.

Discussion

Gold nanoparticles (13 nm) have been previously shown to induce cell death by ROS generation in A549 cells with low intracellular GSH. At higher concentrations, ROS often cause cellular damage, such as ER stress and mitochondrial dysfunction, and then lead to cell death, including apoptosis and necrosis (Basu et al. 2012; Hahm et al. 2011; Steinbrenner and Sies 2009; Verfaillie et al. 2012). In this study, we analyzed the mechanisms involved in GNPs-induced cell death in lung cancer cells with low intracellular GSH.

Changes in actin cytoskeleton dynamics have proved to be crucial for apoptosis. The F-actin depolymerizing agent cytochalasin D rapidly induced the release of cytochrome *c* from mitochondria and caspase activation (Franklin-Tong and Gourlay 2008; Papadopoulou et al. 2008; Paul et al. 2002). Mitochondria play a central role in the life and death of cells. They are not merely the centre for energy metabolism, but are also the headquarters for different catabolic and anabolic processes, calcium fluxes, and various signalling pathways. Mitochondria maintain homeostasis in the cell by interacting with reactive oxygen–nitrogen species and responding adequately to different stimuli (Landes and Martinou 2011; Ni et al. 2012). Ca^{2+} is used by cells as a second messenger required for most biological processes, including proliferation, gene transcription, post-translational modification of proteins, and aerobic metabolism. To exquisitely control and orchestrate this variety of routines, it is mandatory that cells maintain a very low cytosolic Ca^{2+} concentration. Mitochondria can be considered as a firewall that controls the Ca^{2+} concentration in the cell and in cytoplasmic microdomains by tuning the frequency of oscillatory Ca^{2+} signals, and by blunting the spread of cytosolic Ca^{2+} waves. This allows cells to cope with potentially lethal Ca^{2+} loads, which would rapidly activate a variety of degradative enzymes in an uncontrolled fashion (Rasola and Bernardi 2011; Santo-Domingo and Demaurex 2010). Alteration of the ER homeostasis in cancer cells could also be a signal for apoptotic program activation (Pierre et al. 2013). The ER is the major intracellular Ca^{2+} stores of cells. Upon exposure to ER stress, Ca^{2+} can be released from ER to cytoplasm. The accumulation of calcium in the cytoplasm and uptake by the mitochondria causes mitochondria fragmentation, triggering cytochrome *c* release, and thus initiating apoptotic pathway (Wang et al. 2012a). A critical process in apoptosis is the activation of a family of cysteine proteases, termed caspases. Two overlapping caspase-dependent apoptotic pathways have been identified: the death receptor pathway (extrinsic pathway) and the mitochondrial pathway (intrinsic pathway). Both of these pathways converge on caspase-3 activation, eventually resulting in DNA fragmentation (Sayers 2011; Spencer and Sorger 2011). In this study, the activated caspase-dependent apoptosis was detected by measuring the cleaved caspase-3 in GNPs and BSO treated cells by flow cytometry. This observation was consistent with the finding that GNPs induced F-actin disruption, loss of mitochondrial membrane potential, calcium overload, and ER stress. However, the pan caspase inhibitor zVAD-fmk failed to block GNPs-induced cell death as ascertained by annexin v-FITC/PI binding studies. The results indicate that caspase-dependent apoptosis is not the major death pathway induced by GNPs in A549 cells with low intracellular GSH.

DNA DSBs are probably the most dangerous of the many different types of DNA damage that occur within the cell. DSBs are generated by exogenous agents, such as ionizing radiation or by endogenously generated ROS. When exposed to excessive amounts of DNA DSBs that overwhelm their repair machinery, cells will undergo apoptosis (Burma et al. 2001; Sorrells et al. 2012). Within the present study, DNA DSBs were observed in lung cancer cells with low intracellular GSH incubated with GNPs. DNA fragmentation can also occur through the mitochondrial death effector proteins AIF and EndoG. Under some cytotoxic stimuli, both AIF and EndoG are released from the mitochondria and translocated to the nucleus, where they cause DNA fragmentation and caspase-independent apoptosis (Van Loo et al. 2001; Norberg et al. 2010; Saelens et al. 2004; Schneiders et al. 2009; Wang et al. 2012b). In this study, GNPs triggered the translocation of AIF and EndoG to the nucleus. This observation was consistent with the finding that GNPs induced mitochondrial membrane disruption and double stranded DNA breaks. Caspase-independent apoptosis can also be initiated by translocation of glycolytic enzyme GAPDH from the cytoplasm to the nucleus. In the nucleus, GAPDH stabilizes the rapidly turning over Siah1, enhancing its E3 ubiquitin ligase activity, and causes cell death (Hara et al. 2005; Kim et al. 2009). In this study, GAPDH translocated into the nucleus of the cells after GNPs and BSO treatment.

Thus, in the lung cancer cells A549 with low intracellular GSH, GNPs activate caspase-independent cell apoptosis.

The tumor suppressor p53 is a well known regulator of cell division and apoptosis. p53 can mediates cell apoptosis by induction of pro-apoptotic proteins belonging to the Bcl-2 family, such as Bax and PUMA. p53 has also been shown to promote the release of AIF and EndoG from mitochondria. The disequilibrium caused by either upregulation of proapoptotic Bcl-2 family proteins or downregulation of antiapoptotic Bcl-2 family proteins may result in the release of cytochrome *c*, AIF, and EndoG from mitochondria. Cytochrome *c* can activate the caspases and mediate the caspase-dependent apoptosis, while AIF and EndoG trigger cell apoptosis through direct DNA cleavage (Hu et al. 2013; Wang et al. 2012b; Jung et al. 2012). In this study, up-regulation of p53, Bax, and PUMA expression and down-regulation of Bcl-2 expression, are correlated with mitochondrial membrane depolarization, caspase-3 activation and translocation of AIF and EndoG to the nucleus.

Necrosis has been considered a passive, unregulated form of cell death; however, recent evidence indicates that some necrosis can be induced by regulated signal transduction pathways, such as those mediated by receptor interacting protein kinases, especially in conditions, in which caspases are inhibited or cannot be activated efficiently. Both apoptosis and necrosis were observed simultaneously in a wide array of animal and human pathologies, suggesting that apoptosis and necrosis are interconnected, and not entirely separated, events. Caspase inhibition, which distinguishes apoptotic and nonapoptotic cell death, sometimes shifts apoptosis to necrosis or enhances necrosis (Zhang et al. 2009; Trichonas et al. 2010). Our observation that zVAD-fmk did not inhibit, but rather enhanced GNPs-induced cell death in lung cancer cells with low intracellular GSH. Nec-1 has been reported to inhibit caspase-independent necrotic cell death by inhibiting RIP1 kinase. Nec-1 treatment effectively suppresses GNPs-induced cell death in lung cancer cells with low intracellular GSH. These findings suggest that necrosis is an essential mechanism of GNPs-induced cell death.

Acknowledgments The authors thank professor Paul V. Murphy from National University of Ireland (Galway), for critically reviewing the manuscript. This study was supported by the National Natural Science Foundation of China (81102468 to Y. Zhao) and the Natural Science Foundation of Shandong Province (ZR2010HQ063 to Y. Zhao).

Conflict of interest The authors declare that there are no conflicts of interest.

References

Alkilany AM, Murphy CJ (2010) Toxicity and cellular uptake of gold nanoparticles: what we have learned so far? J Nanopart Res 12:2313–2333

Ambrogio MW, Thomas CR, Zhao YL, Zink JI, Stoddart JF (2011) Mechanized silica nanoparticles: a new frontier in theranostic nanomedicine. Acc Chem Res 44:903–913

Basu S, Ganguly A, Chakraborty P, Sen R, Banerjee K, Chatterjee M, Efferth T, Choudhuri SK (2012) Targeting the mitochondrial pathway to induce apoptosis/necrosis through ROS by a newly developed Schiff's base to overcome MDR in cancer. Biochimie 94:166–183

Burma S, Chen BP, Murphy M, Kurimasa A, Chen DJ (2001) ATM phosphorylates histone H2AX in response to DNA double-strand breaks. J Biol Chem 276:42462–42467

Cao R, Jia J, Ma X, Zhou M, Fei H (2013) Membrane localized iridium(III) complex induces endoplasmic reticulum stress and mitochondria-mediated apoptosis in human cancer cells. J Med Chem 56:3636–3644

Dando I, Fiorini C, Pozza ED, Padroni C, Costanzo C, Palmieri M, Donadelli M (2013) UCP2 inhibition triggers ROS-dependent nuclear translocation of GAPDH and autophagic cell death in pancreatic adenocarcinoma cells. Biochim Biophys Acta 1833(3):672–679

Dreaden EC, Mwakwari SC, Austin LA, Kieffer MJ, Oyelere AK, El-Sayed MA (2012) Small molecule-gold nanorod conjugates selectively target and induce macrophage cytotoxicity towards breast cancer cells. Small 8:2819–2822

Erathodiyil N, Ying JY (2011) Functionalization of inorganic nanoparticles for bioimaging applications. Acc Chem Res 44:925–935

Fortes GB, Alves LS, de Oliveira R, Dutra FF, Rodrigues D, Fernandez PL, Souto-Padron T, De Rosa MJ, Kelliher M, Golenbock D, Chan FK, Bozza MT (2012) Heme induces programmed necrosis on macrophages through autocrine TNF and ROS production. Blood 119:2368–2375

Franklin-Tong VE, Gourlay CW (2008) A role for actin in regulating apoptosis/programmed cell death: evidence spanning yeast, plants and animals. Biochem J 413:389–404

Hahm ER, Moura MB, Kelley EE, Van Houten B, Shiva S, Singh SV (2011) Withaferin A-induced apoptosis in human breast cancer cells is mediated by reactive oxygen species. PLoS ONE 6:e23354

Hara MR, Agrawal N, Kim SF, Cascio MB, Fujimuro M, Ozeki Y, Takahashi M, Cheah JH, Tankou SK, Hester LD, Ferris CD, Hayward SD, Snyder SH, Sawa A (2005) S-nitrosylated GAPDH initiates apoptotic cell death by nuclear translocation following Siah1 binding. Nat Cell Biol 7(7):665–674

Ho D, Sun X, Sun S (2011) Monodisperse magnetic nanoparticles for theranostic applications. Acc Chem Res 44: 875–882

Hu X, Xuan Y (2008) Bypassing cancer drug resistance by activating multiple death pathways-A proposal from the study of circumventing cancer drug resistance by induction of necroptosis. Cancer Lett 259:127–137

Hu C, Peng Q, Chen F, Zhong Z, Zhuo R (2010) Low molecular weight polyethylenimine conjugated gold nanoparticles as efficient gene vectors. Bioconjug Chem 21:836–843

Hu W, Ge Y, Ojcius DM, Sun D, Dong H, Yang XF, Yan J (2013) p53 signalling controls cell cycle arrest and caspase-independent apoptosis in macrophages infected with pathogenic Leptospira species. Cell Microbiol. doi:10.1111/cmi.12141

Huang L, Mackenzie GG, Sun Y, Ouyang N, Xie G, Vrankova K, Komninou D, Rigas B (2011) Chemotherapeutic properties of phospho-nonsteroidal anti-inflammatory drugs, a new class of anticancer compounds. Cancer Res 71:7617–7627

Jung HY, Joo HJ, Park JK, Kim YH (2012) The blocking of c-Met signaling induces apoptosis through the increase of p53 protein in lung cancer. Cancer Res Treat 44:251–261

Kang B, Mackey MA, El-Sayed MA (2010) Nuclear targeting of gold nanoparticles in cancer cells induces DNA damage, causing cytokinesis arrest and apoptosis. J Am Chem Soc 132:1517–1519

Kaufmann SH, Lee SH, Meng XW, Loegering DA, Kottke TJ, Henzing AJ, Ruchaud S, Samejima K, Earnshaw WC (2008) Apoptosis-associated caspase activation assays. Methods 44:262–272

Khlebtsov N, Dykman L (2011) Biodistribution and toxicity of engineered gold nanoparticles: a review of in vitro and in vivo studies. Chem Soc Rev 40:1647–1671

Kim JJ, Kim YH, Lee MY (2009) Proteomic characterization of differentially expressed proteins associated with no stress in retinal ganglion cells. BMB Rep 42(7):456–461

Kim D, Jeong YY, Jon S (2010) A drug-loaded aptamer-gold nanoparticle bioconjugate for combined CT imaging and therapy of prostate cancer. ACS Nano 4:3689–3696

Krysko DV, Vanden Berghe T, D'Herde K, Vandenabeele P (2008) Apoptosis and necrosis: detection, discrimination and phagocytosis. Methods 44:205–221

Landes T, Martinou JC (2011) Mitochondrial outer membrane permeabilization during apoptosis: the role of mitochondrial fission. Biochim Biophys Acta 1813:540–545

Li YF, Chen C (2011) Fate and toxicity of metallic and metal-containing nanoparticles for biomedical applications. Small 7:2965–2980

Lu Y, Zhao Y, Yu L, Dong L, Shi C, Hu MJ, Xu YJ, Wen LP, Yu SH (2010) Hydrophilic Co@Au yolk/shell nanospheres: synthesis, assembly, and application to gene delivery. Adv Mater 22:1407–1411

Ma YH, Huang CP, Tsai JS, Shen MY, Li YK, Lin LY (2011) Water-soluble germanium nanoparticles cause necrotic cell death and the damage can be attenuated by blocking the transduction of necrotic signaling pathway. Toxicol Lett 207:258–269

Mazumder S, Plesca D, Almasan A (2008) Caspase-3 activation is a critical determinant of genotoxic stress-induced apoptosis. Methods Mol Biol 414:13–21

Minelli C, Lowe SB, Stevens MM (2010) Engineering nanocomposite materials for cancer therapy. Small 6:2336–2357

Morgan MJ, Liu ZG (2010) Reactive oxygen species in TNF-alpha-induced signaling and cell death. Mol Cells 30:1–12

Mukherjee B, Kessinger C, Kobayashi J, Chen BP, Chen DJ, Chatterjee A, Burma S (2006) DNA-PK phosphorylates histone H2AX during apoptotic DNA fragmentation in mammalian cells. DNA Repair (Amst) 5:575–590

Mura S, Couvreur P (2012) Nanotheranostics for personalized medicine. Adv Drug Deliv Rev 64:1394–1416

Nair RR, Emmons MF, Cress AE, Argilagos RF, Lam K, Kerr WT, Wang HG, Dalton WS, Hazlehurst LA (2009) HYD1-induced increase in reactive oxygen species leads to autophagy and necrotic cell death in multiple myeloma cells. Mol Cancer Ther 8:2441–2451

Ni CH, Yu CS, Lu HF, Yang JS, Huang HY, Chen PY, Wu SH, Ip SW, Chiang SY, Lin JG, Chung JG (2012) Chrysophanol-induced cell death (necrosis) in human lung cancer A549 cells is mediated through increasing reactive oxygen species and decreasing the level of mitochondrial membrane potential. Environ Toxicol. doi:10.1002/tox.21801

Nicotera P (2002) Apoptosis and age-related disorders: role of caspase-dependent and caspase-independent pathways. Toxicol Lett 127:189–195

Norberg E, Orrenius S, Zhivotovsky B (2010) Mitochondrial regulation of cell death: processing of apoptosis-inducing factor (AIF). Biochem Biophys Res Commun 396:95–100

Pan Y, Leifert A, Ruau D, Neuss S, Bornemann J, Schmid G, Brandau W, Simon U, Jahnen-Dechent W (2009) Gold nanoparticles of diameter 1.4 nm trigger necrosis by oxidative stress and mitochondrial damage. Small 5:2067–2076

Papadopoulou N, Charalampopoulos I, Alevizopoulos K, Gravanis A, Stournaras C (2008) Rho/ROCK/actin signaling regulates membrane androgen receptor induced apoptosis in prostate cancer cells. Exp Cell Res 314: 3162–3174

Paul C, Manero F, Gonin S, Kretz-Remy C, Virot S, Arrigo AP (2002) Hsp27 as a negative regulator of cytochrome *C* release. Mol Cell Biol 22:816–834

Pierre AS, Minville-Walz M, Fèvre C, Hichami A, Gresti J, Pichon L, Bellenger S, Bellenger J, Ghiringhelli F, Narce M, Rialland M (2013) Trans-10, cis-12 conjugated linoleic acid induced cell death in human colon cancer cells through reactive oxygen species-mediated ER stress. Biochim Biophys Acta 1831(4):759–768

Rasola A, Bernardi P (2011) Mitochondrial permeability transition in Ca(2+)-dependent apoptosis and necrosis. Cell Calcium 50:222–233

Saelens X, Festjens N, Vande Walle L, van Gurp M, van Loo G, Vandenabeele P (2004) Toxic proteins released from mitochondria in cell death. Oncogene 23:2861–2874

Santo-Domingo J, Demaurex N (2010) Calcium uptake mechanisms of mitochondria. Biochim Biophys Acta 1797:907–912

Sayers TJ (2011) Targeting the extrinsic apoptosis signaling pathway for cancer therapy. Cancer Immunol Immunother 60:1173–1180

Schneiders UM, Schyschka L, Rudy A, Vollmar AM (2009) BH3-only proteins Mcl-1 and Bim as well as endonuclease G are targeted in spongistatin 1-induced apoptosis in breast cancer cells. Mol Cancer Ther 8:2914–2925

Shukla R, Chanda N, Zambre A, Upendran A, Katti K, Kulkarni RR, Nune SK, Casteel SW, Smith CJ, Vimal J, Boote E, Robertson JD, Kan P, Engelbrecht H, Watkinson LD, Carmack TL, Lever JR, Cutler CS, Caldwell C, Kannan R, Katti KV (2012) Laminin receptor specific therapeutic gold nanoparticles (198AuNP-EGCg) show efficacy in treating prostate cancer. Proc Natl Acad Sci USA 109:12426–12431

Sorrells S, Carbonneau S, Harrington E, Chen AT, Hast B, Milash B, Pyati U, Major MB, Zhou Y, Zon LI, Stewart RA, Look AT, Jette C (2012) Ccdc94 protects cells from ionizing radiation by inhibiting the expression of p53. PLoS Genet 8:e1002922

Speirs CK, Hwang M, Kim S, Li W, Chang S, Varki V, Mitchell L, Schleicher S, Lu B (2011) Harnessing the cell death pathway for targeted cancer treatment. Am J Cancer Res 1:43–61

Spencer SL, Sorger PK (2011) Measuring and modeling apoptosis in single cells. Cell 144:926–939

Steinbrenner H, Sies H (2009) Protection against reactive oxygen species by selenoproteins. Biochim Biophys Acta 1790:1478–1485

Trichonas G, Murakami Y, Thanos A, Morizane Y, Kayama M, Debouck CM, Hisatomi T, Miller JW, Vavvas DG (2010) Receptor interacting protein kinases mediate retinal detachment-induced photoreceptor necrosis and compensate for inhibition of apoptosis. Proc Natl Acad Sci USA 107:21695–21700

Umar A, Dunn BK, Greenwald P (2012) Future directions in cancer prevention. Nat Rev Cancer 12:835–848

Van Loo G, Schotte P, van Gurp M, Demol H, Hoorelbeke B, Gevaert K, Rodriguez I, Ruiz-Carrillo A, Vandekerckhove J, Declercq W, Beyaert R, Vandenabeele P (2001) Endonuclease G: a mitochondrial protein released in apoptosis and involved in caspase-independent DNA degradation. Cell Death Differ 8:1136–1142

Verfaillie T, Rubio N, Garg AD, Bultynck G, Rizzuto R, Decuypere JP, Piette J, Linehan C, Gupta S, Samali A, Agostinis P (2012) PERK is required at the ER-mitochondrial contact sites to convey apoptosis after ROS-based ER stress. Cell Death Differ 19(11):1880–1891

Vucic D, Dixit VM, Wertz IE (2011) Ubiquitylation in apoptosis: a post-translational modification at the edge of life and death. Nat Rev Mol Cell Biol 12:439–452

Wang HC, Pao J, Lin SY, Sheen LY (2012a) Molecular mechanisms of garlic-derived allyl sulfides in the inhibition of skin cancer progression. Ann N Y Acad Sci 1271:44–52

Wang L, Liu L, Shi Y, Cao H, Chaturvedi R, Calcutt MW, Hu T, Ren X, Wilson KT, Polk DB, Yan F (2012b) Berberine induces caspase-independent cell death in colon tumor cells through activation of apoptosis-inducing factor. PLoS ONE 7:e36418

Wen L, Chen SJ, Zhang W, Ma HW, Zhang SQ, Chen L (2011) hsBAFF regulates proliferation and response in cultured CD4(+) T lymphocytes by upregulation of intracellular free Ca(2+) homeostasis. Cytokine 53:215–222

Weng HY, Hsu MJ, Chen CC, Chen BC, Hong CY, Teng CM, Pan SL, Chiu WT, Lin CH (2013) Denbinobin induces human glioblastoma multiforme cell apoptosis through the IKKα-Akt-FKHR signaling cascade. Eur J Pharmacol 698:103–109

Xia Y, Li W, Cobley CM, Chen J, Xia X, Zhang Q, Yang M, Cho EC, Brown PK (2011) Gold nanocages: from synthesis to theranostic applications. Acc Chem Res 44:914–924

Zhang DW, Shao J, Lin J, Zhang N, Lu BJ, Lin SC, Dong MQ, Han J (2009) RIP3, an energy metabolism regulator that switches TNF-induced cell death from apoptosis to necrosis. Science 325:332–336

Zhang Y, Zhang G, Hendrix LR, Tesh VL, Samuel JE (2012) *Coxiella burnetii* induces apoptosis during early stage infection via a caspase-independent pathway in human monocytic THP-1 cells. PLoS ONE 7:e30841

Zhao Y, Liu W, Zhou Y, Zhang X, Murphy PV (2010) *N*-(8-(3-ethynylphenoxy)octyl-1-deoxynojirimycin suppresses growth and migration of human lung cancer cells. Bioorg Med Chem Lett 20:7540–7543

Zhao Y, Gu X, Ma H, He X, Liu M, Ding Y (2011) Association of glutathione level and cytotoxicity of gold nanoparticles in lung cancer cells. J Phys Chem C 115:12797–12802